Ubiquitin carboxyl-terminal hydrolase isozyme L1/UCHL1 suppresses epithelial-mesenchymal transition and is under-expressed in cadmium-transformed human bronchial epithelial cells

Wu, Dan-Dan; Xu, Yan-Ming; Chen, De-Ju; Liang, Zhan-Ling; Chen, Xu-Li; Hylkema, Machteld N; Rots, Marianne G; Li, Sheng-Qing; Lau, Andy T Y

Published in:
Cell biology and toxicology

DOI:
10.1007/s10565-020-09560-2

Publication date:
2021

Cell Biol Toxicol (2021) 37:497–513
https://doi.org/10.1007/s10565-020-09560-2

ORIGINAL ARTICLE

Ubiquitin carboxyl-terminal hydrolase isozyme L1/UCHL1 suppresses epithelial–mesenchymal transition and is under-expressed in cadmium-transformed human bronchial epithelial cells

Dan-Dan Wu · Yan-Ming Xu · De-Ju Chen · Zhan-Ling Liang · Xu-Li Chen · Machteld N. Hylkema · Marianne G. Rots · Sheng-Qing Li · Andy T. Y. Lau

Received: 8 June 2020 / Accepted: 23 September 2020 / Published online: 10 October 2020

Abstract Cadmium (Cd), a highly toxic heavy metal, is widespreadly distributed in the environment. Chronic exposure to Cd is associated with the development of several diseases including cancers. Over the decade, many researches have been carried on various models to examine the acute effects of Cd; yet, limited knowledge is known about the long-term Cd exposure, especially in the human lung cells. Previously, we showed that chronic Cd-exposed human bronchial epithelial BEAS-2B cells exhibited transformed cell properties, such as anchorage-independent growth, augmented cell migration, and epithelial–mesenchymal transition (EMT). To study these Cd-transformed cells more comprehensively, here, we further characterized their subproteomes. Overall, a total of 63 differentially expressed proteins between Cd-transformed and passage-matched control cells among the five subcellular fractions (cytoplasmic, membrane, nuclear-soluble,

Dan-Dan Wu and Yan-Ming Xu contributed equally to this work.

Graphical headlights
- Subcellular proteomeanalysis was conducted to identify global changes in the protein expressionprofiles of chronic cadmium-exposed human bronchial epithelial BEAS-2B cells
- UCHL1 is under-expressed incadmium-transformed human BEAS-2B cells
- We found that loss of UCHL1plays a function on EMT in these cells

Electronic supplementary material The online version of this article (https://doi.org/10.1007/s10565-020-09560-2) contains supplementary material, which is available to authorized users.

D.-D. Wu · Y.-M. Xu · D.-J. Chen · Z.-L. Liang · X.-L. Chen · A. T. Y. Lau (✉)
Laboratory of Cancer Biology and Epigenetics, Department of Cell Biology and Genetics, Shantou University Medical College, Shantou 515041 Guangdong, People's Republic of China
e-mail: andytylau@stu.edu.cn

D.-D. Wu · M. N. Hylkema · M. G. Rots
Department of Pathology and Medical Biology, University of Groningen, University Medical Center Groningen, 9713 GZGroningen, The Netherlands

D.-D. Wu · M. N. Hylkema
GRIAC Research Institute, University of Groningen, University Medical Center Groningen, 9713 GZGroningen, The Netherlands

S.-Q. Li
Department of Pulmonary and Critical Care Medicine, Huashan Hospital, Fudan University, Shanghai 200040, People's Republic of China

chromatin-bound, and cytoskeletal) were identified by mass spectrometric analysis and database searching. Interestingly, we found that the thiol protease ubiquitin carboxyl-terminal hydrolase isozyme L1 (UCHL1) is one of the severely downregulated proteins in the Cd-transformed cells. Notably, the EMT phenotype of Cd-transformed cells can be suppressed by forced ectopic expression of UCHL1, suggesting UCHL1 as a crucial modulator in the maintenance of the proper differentiation status in lung epithelial cells. Since EMT is considered as a critical step during malignant cell transformation, finding novel cellular targets that can antagonize this transition may lead to more efficient strategies to inhibit cancer development. Our data report for the first time that UCHL1 may play a function in the suppression of EMT in Cd-transformed human lung epithelial cells, indicating that UCHL1 might be a new therapeutic target for chronic Cd-induced carcinogenesis.

Keywords BEAS-2B · Chronic cadmium exposure · Human lung cells · Subcellular proteomics · Ubiquitin carboxyl-terminal hydrolase isozyme L1 · Epithelial–mesenchymal transition

Introduction

Cadmium (Cd) is a carcinogenic toxic metal classified by the International Agency for Research on Cancer (IARC 1993). Cd exposure is a major concern for public health according to WHO reports (2010). Although Cd is uncommon in the natural environment, it is widely used in industrial products, such as batteries, fluorescence microscopes, electroplating, and various pigment products (Kawasaki et al. 2004; Kim et al. 2015). The industrial activities lead to comparatively high accumulation of Cd through the biomagnification of the food chain which is exposed to Cd-contaminated soil and water (Kim et al. 2015). Cd is considered as one of the main carcinogenic components of tobacco through hyper-accumulation in tobacco leaves, and tobacco smoking is another main cause of Cd exposure (Satarug and Moore 2004; Scherer and Barkemeyer 1983). Inhaled Cd oxide during tobacco smoking is likely to deposit in lung tissues and/or the blood circulation (Ganguly et al. 2018; Satarug and Moore 2004). As a component of tobacco, Cd has proven to cause pulmonary inflammation and emphysema via pulmonary oxidative stress in rats model (Kirschvink et al. 2006; Nair et al. 2013). Although consistent reports have pointed out the association between Cd exposure and lung-related diseases, very little is known about the underlying mechanism and progression.

Our group has been investigating the molecular mechanisms of Cd-induced cytotoxicity, adaptation, and carcinogenesis, and aiming to discover potential therapeutic targets for cancer intervention. Our previous results indicated that the acquisition of death tolerance in Cd-resistant rat lung epithelial cells was associated with basal metallothionein levels, perturbation of the JNK pathway, and overexpression of cytokeratin 8/14 (Lau and Chiu 2007). We also found that the expression of metal transporter Zip8 was drastically decreased in Cd-resistant lung epithelial cells from rat, indicating that during chronic Cd exposure, downregulation of Zip8 was involved in the adaptive cell survival mechanism (Gao et al. 2017). To further investigate the underlying mechanism of chronic Cd exposure on human lung epithelium, we established a Cd-adapted human bronchial epithelial BEAS-2B cell model. Cd-sensitive cells were chronically exposed to a stepwise increase of cadmium chloride ($CdCl_2$) concentrations by mimicking chronic Cd exposure in the environment. Recently, we found that Cd-adapted cells exhibited transformed cell properties (augmented cell migration ability and soft agar–based anchorage-independent growth) and aberrant histone modifications (Liang et al. 2018). In addition, we found that post-chronic Cd exposure is closely associated with differential gene expression profiles of DNA damage and DNA repair in human bronchial epithelial cells (Tan et al. 2019).

Our previous research mainly covered the Cd-induced epigenotoxicity by global epiproteomic interrogation; however, in this study, we specifically focused on exploring the proteome profiles of human bronchial epithelial cells responding to chronic Cd exposure. Whole cell proteomics, with all the extracted proteins resolving on the same gel, make the spots difficult to be separated if the proteins are of similar pI and molecular size. Therefore, to improve the resolution and simplify the mixture of proteins obtained from the cells, subcellular fractionation was performed to isolate individual fractions prior to 2-D gel electrophoresis, which reduced the sample complexity while enhancing the resolving capability (Lee et al. 2010; Tan et al. 2018). Also, compared with traditional whole cell proteomics, subcellular proteomics can delineate the subcellular locations of protein. In this current study, we investigate the

subproteome profiles of Cd-transformed human bronchial epithelial cells using 2-D gel electrophoresis preceded by subcellular fractionation. We identified a list of differentially expressed proteins in Cd-transformed cells and found that the ubiquitin carboxyl-terminal hydrolase isozyme L1 (UCHL1), a member of the ubiquitin C-terminal hydrolase (UCH) class of deubiquitinase family, was markedly decreased in Cd-transformed cells. We showed that the low expression of UCHL1 was likely resulted from DNA methylation and histone deacetylation. Further functional studies demonstrated that the epithelial–mesenchymal transition (EMT) phenotype of Cd-transformed cells could be reverted through forced ectopic expression of UCHL1. Moreover, the ubiquitylation changes in Cd-transformed cells were explored, and we showed that 23 ubiquitylated proteins were altered. The current findings offer new insights into the novel role of UCHL1 in the process of lung epithelial cell differentiation under chronic Cd exposure, indicating that UCHL1 might be a new therapeutic target for chronic Cd-induced carcinogenesis.

Materials and methods

Reagents

The chemicals $CdCl_2$, 5-aza-2′-deoxycytidine (5-Aza-dC) and trichostatin A (TSA) were purchased from Sigma-Aldrich (St. Louis, MO, USA). The MS-275 was obtained from Selleck (Shanghai, China). The general reagents, including the protein clean-up kit, silver staining kits, and other proteome analysis reagents, used in this study were obtained from GE Healthcare (Uppsala, Sweden) and Sigma-Aldrich. Primary antibodies used for immunoblot analysis were obtained from GeneTex (Irvine, CA, USA), Santa Cruz Biotechnology (Santa Cruz, CA, USA), Sangon Biotech (Shanghai, China), and Cell Signaling Technology (Danvers, MA, USA), the detailed information is listed in supplemental Table S1.

Human lung cell model for chronic Cd exposure

The Cd-transformed human bronchial epithelial cells and passage-matched control were generated as we described previously (Liang et al. 2018). Briefly, the BEAS-2B cell line (CRL-9609) was purchased from the American Type Culture Collection (Rockville, MD, USA). BEAS-2B cells were cultured in LHC-9 medium at 37 °C in an atmosphere containing 5% CO_2 and 95% air according to manufacturer's instruction. LHC-9 was prepared with LHC basal medium (Gibco, Grand Island, NY) supplemented with other growth factors, cytokines, and solutions as previously described (Liang et al. 2018). BEAS-2B cells were gradually challenged with an increasing dose of $CdCl_2$ (ranging from 1 to 20 μM) in LHC-9 medium for around 20 passages. The obtained Cd resistant cells were further applied to a soft agar-based anchorage-independent growth assay, and clones were then pooled together and designated as T20 cells (Liang et al. 2018) and sham-exposed BEAS-2B control cells were named as passage-matched (PM).

Cell culture of primary bronchial epithelial cells

Human primary bronchial epithelial cells (PBECs) (n = 4) were collected from tracheal tissue of transplant donors from the University Medical Center Groningen. No further information was available from these donors. PBECs were grown on fibronectin/collagen pre-coated plates in keratinocyte serum–free medium (KSFM, Gibco) complemented with 0.2 ng/ml epidermal growth factor, 25 μg/ml bovine pituitary extract, and 1 μM isoproterenol.

Exposure to epigenetic inhibitors

For the treatment of epigenetic inhibitors to Cd-transformed BEAS-2B cells, T20 cells were sham-exposed or challenged with 5–10 μM of 5-Aza-dC or 1–3 μM of MS-275, respectively, for 48 h. An equal amount of DMSO was added as control for both the treatments of 5-Aza-dC and MS-275. Cells were harvested and subjected to immunoblot assay.

For the exposure of epigenetic inhibitors to PBECs, PBECs were seeded onto pre-coated plates and sham-exposed or challenged with 5–10 μM of 5-Aza-dC or 0.5–1 μM of TSA, respectively, for 24 h when the cells were at 80% confluence. Cells were collected for RNA isolation and quantitative real-time RT-PCR was performed to determine UCHL1 mRNA expression.

2-DE-MS analysis

To investigate the subproteome profiles of human bronchial epithelial cells upon chronic Cd exposure,

subcellular proteins were isolated and applied for 2-D PAGE and MS analysis. The cytoplasmic, membrane, nuclear-soluble, chromatin-bound, and cytoskeletal fractions were extracted from PM control and Cd-transformed BEAS-2B cells with the Subcellular Protein Fractionation Kit for Cultured Cells (Pierce Thermo Scientific, Rockford, IL) following the manufacturer's protocol. For 2-D PAGE, subcellular fractions were further purified by employing the Plus One 2-D Clean-Up kit (Bio-Rad). Equal amounts of subcellular proteins following clean-up were subjected to 2-D gel electrophoresis through Ettan IPG phor 3 IEF (isoelectric focusing) system (GE Healthcare) and Hoefer SE 600 electrophoresis units as previously described (Xu et al. 2019). After 2-D gel electrophoresis, ImageScanner III from GE Healthcare was applied to scan the silver staining gels and PDQuest software from Bio-Rad was used to analyze the gel images and quantify the intensity of protein spots. Only spots with a fold change ≥ 1.3 and spots which either appeared or vanished were excised from the gels and applied for MS analysis.

GO annotation and bioinformatic analysis

Gene ontology (GO) enrichment analysis was used to investigate the biological significance of differentially expressed proteins identified from MS analysis using the Database for Annotation, Visualization, and Integrated Discovery (DAVID) as previously described (Xu et al. 2019). All GO terms within the cellular component, molecular function, or biological process were arranged according to the $-\log_{10}(p)$ values, which was considered to be significant when the $-\log_{10}(p)$ level was more than 1.3 (which is $p \leq 0.05$).

RNA isolation and conditions for RT-PCR

Total RNA from cells was isolated using TRIzol reagent (Thermo Fisher Scientific; 15596018) in accordance with the manufacturer's instruction. cDNA synthesis was performed using PrimeScript Reverse Transcriptase (Takara, Dalian, China; 2680A) following the manufacturer's protocol, supplemented with random hexamer primers. Expression of UCHL1 in PM and T20 cells was measured using RT-PCR and quantitative real-time RT-PCR with gene-specific primers obtained from Beijing Genomics Institute (Shenzhen, China). β-Actin/GAPDH was monitored as an internal control. mRNA expression of UCHL1 in PBECs treated with epigenetic inhibitors were assessed by quantitative real-time RT-PCR. Fold changes in mRNA expression compared to control were calculated by comparative Ct method ($2^{-\Delta\Delta Ct}$ method) after normalization to GAPDH expression (Livak and Schmittgen 2001). At least three biological repeats were done for quantitative real-time RT-PCR. Gene-specific primers used are listed at Table S2.

Construction of plasmid and stable cell lines

Human UCHL1 full-length cDNA (669 bp) was amplified from BEAS-2B cDNA and inserted into pcDNA4/HisMaxA at *Bam*H I and *Xba* I sites to generate the pcDNA4/Xpress-UCHL1. The recombinant plasmid was validated by DNA sequencing from Beijing Genomics Institute.

For the generation of stably UCHL1 expressing cells, pcDNA4/Xpress-UCHL1 or its empty vector control were transfected into T20 cells via Lipofectamine 2000 (Invitrogen) following the manufacturer's suggested instruction. At 24 h post-transfection, cells were selected with Zeocin for 14 days. The ectopic overexpression of UCHL1 was confirmed by immunoblot assay.

Immunoblot assay

Briefly, equal amounts of proteins were resolved by proper percents of sodium dodecyl sulfate polyacrylamide gels and electrotransferred onto PVDF membranes. The membranes were blocked with 5% (w/v) non-fat dry milk in Tris-buffered saline (TBS) and incubated with varieties of detection antibodies. Subsequently, the membranes were washed thrice with TBS containing 0.1% Tween 20 for 10 min and incubated with the indicated secondary antibodies. After washing, proteins were visualized with the chemiluminescence (Tanon 5200, Shanghai, China). The intensity of the target bands were quantified by Gel-Pro Analyzer 4 and expressed as relative ratios. Each experiment was performed thrice independently and representative data are shown.

Cell migration assays

For the wound healing-based cell migration assay, equal numbers of BEAS-2B stable cell lines were seeded into dishes and a wound was scratched using a pipette tip

when the confluence of cells reached 90–95%. Subsequently, cells were washed with DPBS thrice to get rid of cell debris, then renewed with fresh LHC-9 growth medium and cultured for another 24 h. After incubation, migrated cells were photographed by a phase contrast microscope. The cell migration ability of the scratched wound field was measured by the Image-Pro Plus software through subtracting the width (area/length) of the wound at 24 h from 0 h.

For the transwell-based cell migration assay, the procedure was conducted as previously described (Liang et al. 2018). Briefly, cells suspended in LHC basic medium containing 10% LHC-9 complete growth medium were seeded into Costar Transwell chambers (Corning, NY), and the bottom well was placed with 600 μL LHC-9 complete growth medium. After 40 h incubation, the inserts were washed with DPBS thrice and fixed with methanol for 20 min. The migrated cells were stained with crystal violet (0.1%) for 15 min while cells maintained in the transwells were wiped off using a cotton swab. The transwells were air-dried and then photographed using the phase contrast microscope. Five spots from each chamber were examined. The number of migrated cells was counted manually from five spots of each transwell.

Ubiquitin array analysis

Ubiquitylation changes were determined in PM and T20 cells using the Human Ubiquitin Array Kit obtained from R&D Systems (Minneapolis, MN; ARY027). Analysis of ubiquitylation was conducted following the manufacturer's protocols. In short, cells were harvested and washed with PBS after treatment and lysed with Lysis buffer 6. The cell extracts were resuspended and rotated for 30 min at 4 °C, then microcentrifuged for 5 min, and the supernatant was subjected to protein quantification. The array membrane, provided from the kit, was incubated with blocking buffer for 1 h on a shaker. The array membranes were then incubated with protein lysates at 4 °C, overnight. After incubation, the membranes were rinsed with provided washing buffer, thrice, for 10 min. The array membranes were incubated with detection antibodies for 1 h and then washed thrice with washing buffer. Streptavidin-HRP solution was subsequently added to the array membranes and incubated for 30 min and the membranes were washed thrice with washing buffer. Protein spots on the array membrane were visualized through Chemi Reagent Mix provided in the kit. The gray intensity of each spot was determined via the ImageJ software and the fold change relative to PM control was adjusted by subtracting the averaged background signal. The corresponding list of antibodies is indicated in Table S3.

Statistical analysis

Statistical analysis was done using the GraphPad Prism® 8 software (GraphPad Software Inc.). All quantitative results were presented as means of biological repeats as indicated and analyzed using one-way ANOVA. Unless stated otherwise, the reproducibility was performed in at least thrice independently and one of the results was shown, as repeats showed similar trends. A two-tailed Student's *t* test was applied to analyze the significant differences. A $p \leq 0.05$ was considered significant.

Results

Subproteome profiles of Cd-transformed and passage-matched control cells

Previously, epiproteome profiling of human bronchial epithelial BEAS-2B cells chronically exposed to $CdCl_2$ was performed to identify the epigenotoxicity of chronic Cd exposure (Liang et al. 2018). In the current study, we continued to explore the proteome profiles of human bronchial epithelial cells exposed chronically to Cd. Since subcellular proteomics allows us to assess proteins more sensitively and specifically from organelles of interest (Tan et al. 2018), cells were firstly subjected to subcellular fractionation prior to electrophoresis. Each of the subcellular portions was analyzed via immunoblot with antibodies against each subcellular extraction, which include cytoplasmic (RELA), membrane (DMT-1), nuclear-soluble (SP1), chromatin-bound (histone H3), and cytoskeletal (cytokeratin 7). The results demonstrate that pure subcellular fractionation with low cross contamination was achieved, which allowed for the subsequent 2-D PAGE analysis (Fig. S1).

Next, the five subcellular protein samples extracted from PM and T20 cells were subjected to gel-based proteomics (Fig. S2a-e) and differentially expressed spots were identified by PDQuest software analysis; spots are shown in montage view (Fig. 1). Then, MS identification of aberrantly expressed protein spots were

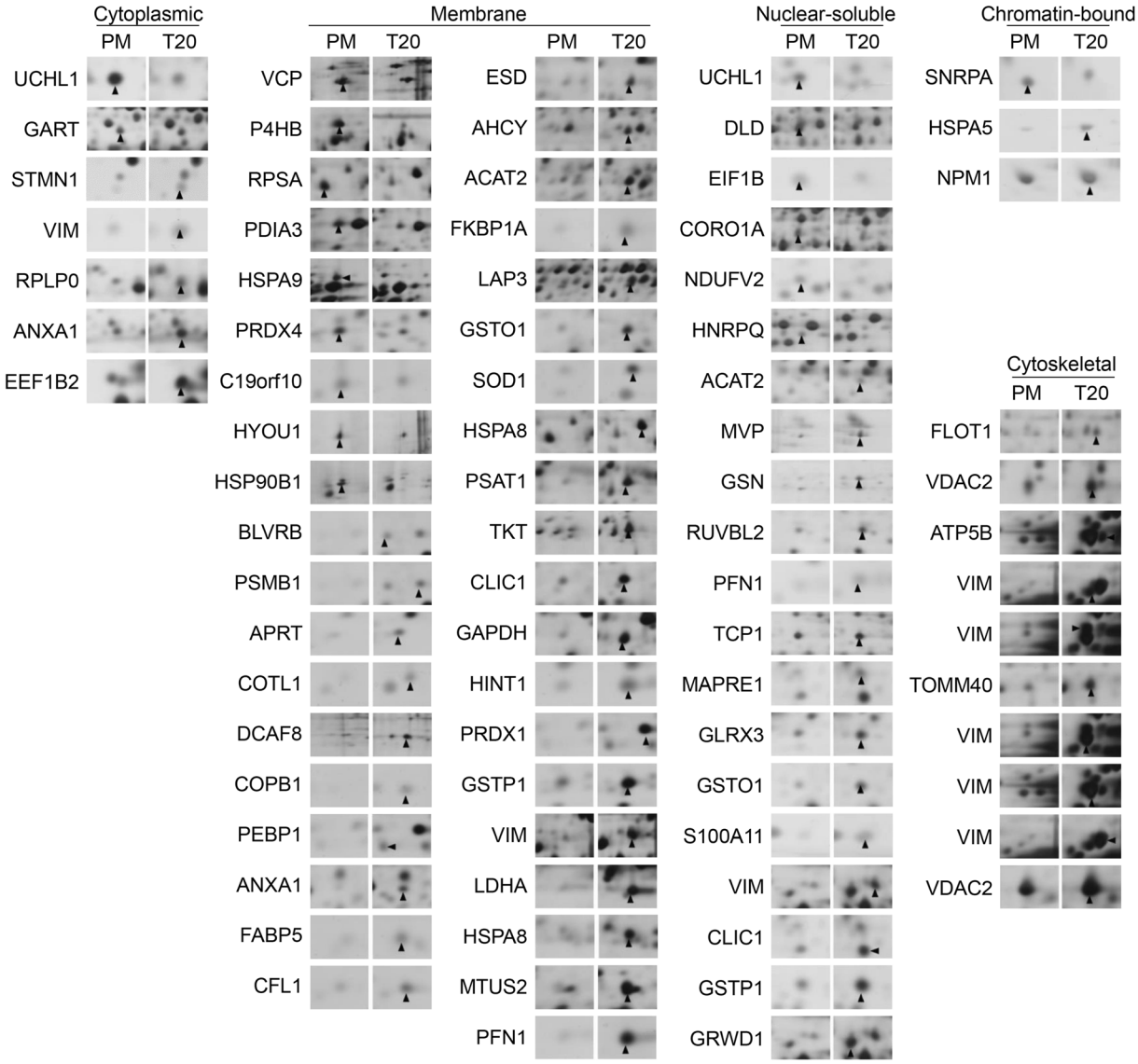

Fig. 1 Montage view of 2-D gel spots. Dysregulation of protein expression from five subcellular fractions between Cd-adapted and passage-matched BEAS-2B cells was assessed by a two-dimensional PAGE and identified by MS analysis as shown in montage view

obtained after excision and trypsin digestion. The 79 proteins identified based on database searching are shown in Table 1, and the expression levels of each identified proteins between T20 and PM are summarized in Fig. 2 and Table S4. In general, there was marked upregulation of glutathione S-transferases (GST, the enzyme involved in the glutathione metabolic process, like GSTP1 and GSTO1), and altered expression of antioxidant enzymes (for example, SOD1, PRDX1, and PRDX4), protein disulfide isomerase (PDI) gene family member (such as PDIA3 and P4HB/PDIA1), proteins associated with cell migration (such as VIM, GSN, and CFL1) and heat shock proteins (HSP, such as HSP90B1 and heat shock protein 70 family members including HSPA5, HSPA8, HSPA9, and HYOU1). Moreover, several aberrantly expressed proteins between T20 and PM identified by MS were further confirmed by immunoblot analysis with whole cell lysates (Fig. S3), which showed a similar trend of expression (up/downregulation) as in 2-D electrophoresis, indicating that the results of the MS analysis are reliable.

Table 1 Identification of aberrantly-expressed proteins between passage-matched and Cd-transformed BEAS-2B cells. Protein spots were quantified after 2-D PAGE and identified by MS and protein database searching. The up/downregulation of proteins as compared with passage-matched is indicated by arrows among the five subcellular fractions.

Sample number	Abbreviation	Protein name	Accession no.	pI	MW (kDa)	Matched peptide	Coverage (%)	Mascot score
Cytoplasmic								
1	UCHL1	Ubiquitin carboxyl-terminal hydrolase isozyme L1 ↓	P09936	5.22	24.8	10	36.3	3204
2	GART	Trifunctional purine biosynthetic protein adenosine-3 ↓	P22102	6.27	107.8	17	15.7	2430
3	STMN1	Stathmin ↑	P16949	5.76	17.3	7	44.3	1195
4	VIM	Vimentin ↑	P08670	5.05	53.7	5	10.3	168
5	RPLP0	60S acidic ribosomal protein P0 ↑	P05388	5.70	34.3	13	43.9	2159
6	ANXA1	Annexin A1 ↑	P04083	6.64	38.7	11	28.9	829
7	EEF1B2	Elongation factor 1-beta ↑	P24534	4.50	24.8	7	35.1	940
Membrane								
8	VCP	Transitional endoplasmic reticulum ATPase ↓	P55072	5.14	89.3	16	25.3	2384
9	P4HB	Protein disulfide-isomerase ↓	P07237	4.69	57.1	4	8.5	402
10	RPSA	40S ribosomal protein SA ↓	P08865	4.79	32.9	7	25.4	3325
11	PDIA3	Protein disulfide-isomerase A3 ↓	P30101	5.61	56.8	4	7.7	85
12	HSPA9	Stress-70 protein, mitochondrial ↓	P38646	5.44	73.7	5	10.5	304
13	PRDX4	Peroxiredoxin-4 ↓	Q13162	5.86	30.5	3	10.7	451
14	C19orf10	UPF0556 protein C19orf10 ↓	Q969H8	6.22	18.8	5	20.8	664
15	HYOU1	Hypoxia up-regulated protein 1 ↓	Q9Y4L1	5.16	111.3	2	2.7	41
16	HSP90B1	Endoplasmin ↓	P14625	4.73	92.5	8	11.3	1024
17	BLVRB	Flavin reductase (NADPH) ↑	P30043	7.31	22.1	4	17.5	436
18	PSMB1	Proteasome subunit beta type-1 ↑	P20618	8.32	26.5	7	27	723
19	APRT	Adenine phosphoribosyltransferase ↑	P07741	5.77	19.6	9	5.6	128
20	COTL1	Coactosin-like protein ↑	Q14019	5.51	15.9	2	13.4	116
21	DCAF8	DDB1- and CUL4-associated factor 8 ↑	Q5TAQ9	5.21	66.9	1	1.8	37
22	COPB1	Coatomer subunit beta ↑	P53618	5.72	107.1	1	1.2	38
23	PEBP1	Phosphatidylethanolamine-binding protein 1 ↑	P30086	7.43	21.1	5	31.6	1126
24	ANXA1	Annexin A1 ↑	P04083	6.64	38.7	4	16.5	713
25	FABP5	Fatty acid-binding protein, epidermal ↑	Q01469	6.82	15.2	5	36.3	335
26	CFL1	Cofilin-1 ↑	P23528	8.26	18.5	2	15.1	175
27	ESD	S-formylglutathione hydrolase ↑	P10768	6.58	31.5	7	24.5	656
28	AHCY	Adenosylhomocysteinase ↑	P23526	5.92	47.7	11	23.4	1210
29	ACAT2	Acetyl-CoA acetyltransferase, cytosolic ↑	Q9BWD1	6.46	41.4	9	21.7	400
30	FKBP1A	Peptidyl-prolyl cis-trans isomerase FKBP1A ↑	P62942	8.08	12.0	3	25	487
31	LAP3	Cytosol aminopeptidase ↑	P28838	8.03	56.2	10	24.5	1296
32	GSTO1	Glutathione S-transferase omega-1 ↑	P78417	6.23	27.6	12	40.7	1759
33	SOD1	Superoxide dismutase [Cu-Zn] ↑	P00441	5.70	15.9	1	9.1	235
34	HSPA8	Heat shock cognate 71 kDa protein ↑	P11142	5.37	70.9	7	10.8	947
35	PSAT1	Phosphoserine aminotransferase ↑	Q9Y617	7.56	40.4	20	47.6	3803
36	TKT	Transketolase ↑	P29401	7.58	67.9	20	29.9	2012
37	CLIC1	Chloride intracellular channel protein 1 ↑	O00299	5.09	26.9	4	23.2	1038
38	GAPDH	Glyceraldehyde-3-phosphate dehydrogenase ↑	P04406	8.58	36.0	5	20	2347
39	HINT1	Histidine triad nucleotide-binding protein 1 ↑	P49773	6.46	13.8	2	12.7	195

Table 1 (continued)

Sample number	Abbreviation	Protein name	Accession no.	pI	MW (kDa)	Matched peptide	Coverage (%)	Mascot score
40	PRDX1	Peroxiredoxin-1 ↑	Q06830	8.27	22.1	10	44.7	1789
41	GSTP1	Glutathione S-transferase P ↑	P09211	5.44	23.4	6	39.1	816
42	VIM	Vimentin ↑	P08670	5.05	53.7	9	22.3	668
43	LDHA	L-lactate dehydrogenase A chain ↑	P00338	8.46	36.7	13	36.5	3171
44	HSPA8	Heat shock cognate 71 kDa protein ↑	P11142	5.37	70.9	13	20	1906
45	MTUS2	Microtubule-associated tumor suppressor candidate 2 ↑	Q5JR59	6.23	150.2	1	0.5	37
46	PFN1	Profilin-1 ↑	P07737	8.47	15.1	9	62.9	3005
Nuclear-soluble								
47	UCHL1	Ubiquitin carboxyl-terminal hydrolase isozyme L1 ↓	P09936	5.22	24.8	5	29.6	483
48	DLD	Dihydrolipoyl dehydrogenase, mitochondrial ↓	P09622	6.50	54.2	5	13	836
49	EIF1B	Eukaryotic translation initiation factor 1b ↓	O60739	6.82	12.8	1	12.4	160
50	CORO1A	Coronin-1A ↓	P31146	6.25	51.0	8	17.1	575
51	NDUFV2	NADH dehydrogenase [ubiquinone] flavoprotein 2, mitochondrial ↓	P19404	5.71	27.4	8	36.5	864
52	HNRPQ	Heterogeneous nuclear ribonucleoprotein Q ↓	O60506	8.68	69.6	7	11.9	322
53	ACAT2	Acetyl-CoA acetyltransferase, cytosolic ↑	Q9BWD1	6.46	41.4	1	5	40
54	MVP	Major vault protein ↑	Q14764	5.34	99.3	33	42.2	5408
55	GSN	Gelsolin ↑	P06396	5.72	85.7	17	27.6	2612
56	RUVBL2	RuvB-like 2 ↑	Q9Y230	5.49	51.2	19	38.9	3466
57	PFN1	Profilin-1 ↑	P07737	8.47	15.0	6	55.7	888
58	TCP1	T-complex protein 1 subunit alpha ↑	P17987	5.80	60.3	24	47.3	6002
59	MAPRE1	Microtubule-associated protein RP/EB family member 1 ↑	Q15691	5.02	30.0	8	25	980
60	GLRX3	Glutaredoxin-3 ↑	O76003	5.31	37.4	9	30.5	997
61	GSTO1	Glutathione S-transferase omega-1 ↑	P78417	6.24	27.6	1	5.8	145
62	S100A11	Protein S100-A11 ↑	P31949	6.82	11.7	4	34.3	685
63	VIM	Vimentin ↑	P08670	5.05	53.7	10	21.2	975
64	CLIC1	Chloride intracellular channel protein 1 ↑	O00299	5.09	26.9	16	76.3	4004
65	GSTP1	Glutathione S-transferase P ↑	P09211	5.44	23.4	13	61.4	5581
66	GRWD1	Glutamate-rich WD repeat-containing protein 1 ↑	Q9BQ67	4.82	49.4	4	13.7	221
Chromatin-bound								
67	SNRPA	U1 small nuclear ribonucleoprotein A ↓	P09012	9.83	31.3	7	30.5	847
68	HSPA5	78 kDa glucose-regulated protein ↑	P11021	5.01	72.3	27	40.5	6755
69	NPM1	Nucleophosmin ↑	P06748	4.64	32.6	14	40.8	5865
Cytoskeletal								
70	FLOT1	Flotillin-1 ↑	O75955	7.08	47.4	18	43.6	2771
71	VDAC2	Voltage-dependent anion-selective channel protein 2 ↑	P45880	7.66	31.6	7	30.6	2600
72	ATP5B	ATP synthase subunit beta, mitochondrial ↑	P06576	5.26	56.7	16	30.1	2737
73	VIM	Vimentin ↑	P08670	5.05	53.7	34	56.7	14,995
74	VIM	Vimentin ↑	P08670	5.05	53.7	40	64.8	18,884
75	TOMM40	Mitochondrial import receptor subunit TOM40 homolog ↑	O96008	6.79	37.9	11	29.9	2603

Table 1 (continued)

Sample number	Abbreviation	Protein name	Accession no.	pI	MW (kDa)	Matched peptide	Coverage (%)	Mascot score
76	VIM	Vimentin ↑	P08670	5.05	53.7	44	71.7	27,568
77	VIM	Vimentin ↑	P08670	5.05	53.7	41	66.5	27,120
78	VIM	Vimentin ↑	P08670	5.05	53.7	38	64.4	11,918
79	VDAC2	Voltage-dependent anion-selective channel protein 2 ↑	P45880	7.66	31.6	11	52	4778

Protein network analysis of differentially expressed proteins from chronic Cd-exposed cells

Next, GO enrichment analysis based on DAVID database was performed to analyze the differentially expressed proteins between PM and T20. We found that the aberrantly expressed proteins upon chronic Cd exposure were closely associated with the categories of cell-cell adherens junction, cell redox homeostasis, and ubiquitin protein ligase binding (Fig. 3). Especially, the marked upregulation of adherens junction-related proteins, such as PFN1, HSPA8, S100A11, LDHA, ANXA1, CLIC1, PRDX1, HSPA5, FLOT1, and MAPRE1, is likely to promote cell-cell/anchoring junction and further contribute to cell survival. Furthermore, the upregulation of redox-associated proteins, such as GST family members (GSTP1 and GSTO1) and antioxidant enzymes (SOD1 and PRDX1) that are responsible for the detoxification of reactive oxygen species (ROS), are supposed to be involved in the maintenance of cell redox homeostasis upon chronic Cd exposure. Interestingly, decreased expression of proteins related to ubiquitin protein ligase binding, including UCHL1 and VCP (which contribute to substrate degradation through the

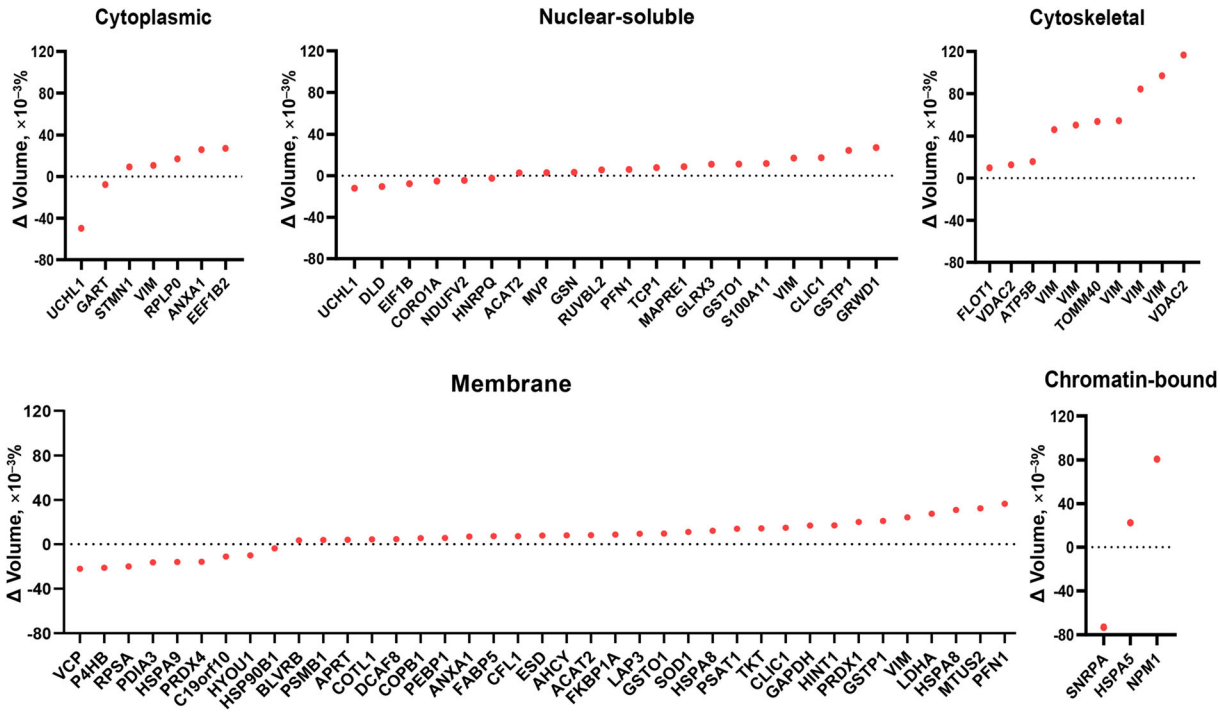

Fig. 2 The five dot plots showing the aberrant expression of a total of 79 spots (63 different protein types) from five subcellular fractions identified by 2-DE analysis. The expression level for each spot was quantified using PDQuest software and expressed in Δ volume ($\times 10^{-3}$%) through subtracting PM from T20. Data were arranged from the lowest value to the highest (left to right) based on mean value as indicated

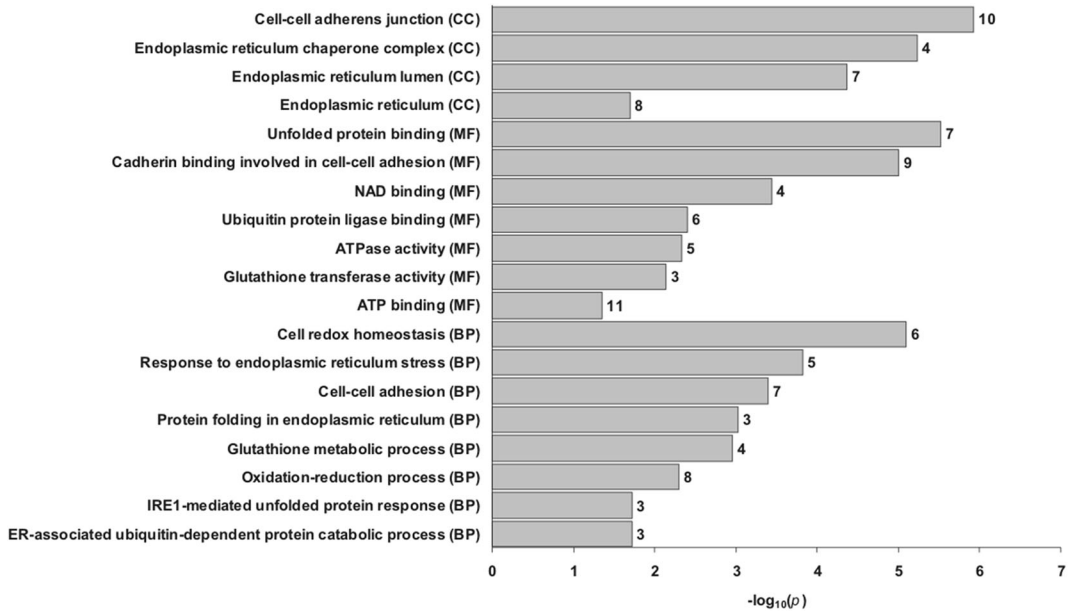

Fig. 3 Bioinformatic analysis of 63 protein types by DAVID. Gene ontology (GO) enrichment analysis was performed to analyze the identified proteins using DAVID. The $-\log_{10}(p)$ level more than 1.3 (which is $p \leq 0.05$) was considered to be significant and included in this figure. All GO categories within the same molecular function or biological process were arranged according to the $-\log_{10}(p)$ values. The number of proteins within each GO category was labeled at the right side of each GO term. CC, cellular component; MF, molecular function; BP, biological process

ubiquitin-proteasome system), was found in T20 cells. These data suggest that various cell activities happened to maintain the cell homeostasis and struggle from cell death upon Cd stress.

UCHL1 expression is correlated to cell migration

The loss of tumor suppressor expression commonly occurs during the process of malignant transformation. Intriguingly, the expression of UCHL1 was downregulated most dramatically in cytoplasmic and nuclear fractions in Cd-transformed BEAS-2B cells according to the Δ volume quantified by specialized PDQuest software from Bio-Rad (Fig. 2); also, UCHL1 was decreased markedly in whole cell lysates (Fig. S3). Therefore, we focused on UCHL1 for further study. Since UCHL1 has been demonstrated as a tumor suppressor in several cancers because of its silencing (Mandelker et al. 2005; Okochi-Takada et al. 2006; Yamashita et al. 2006; Kagara et al. 2008; Tokumaru et al. 2008; Yu et al. 2008; Li et al. 2010; Ummanni et al. 2011; Jin et al. 2013; Tian et al. 2013; Abdelmaksoud-Dammak et al. 2016; Zhao et al. 2020), here we asked the possible role of UCHL1 silencing could play in the pathological process of chronic Cd exposure. As we previously

Fig. 4 Influence of UCHL1 on the cell migratory ability of human lung epithelial cells. **a** The expression of UCHL1 in T20 mock cells and T20 cells stably expressing UCHL1. Immunoblot analysis was used to measure the expression of UCHL1 using antibodies against UCHL1. **b** A wound was scratched in T20 mock cells and T20 cells stably expressing UCHL1 when the cell confluence reached 90–95% and medium were renewed with fresh LHC-9 medium. Photos were taken at 0 and 24 h under light microscope, and the cell migration distance in the wound field was calculated by the Image-Pro Plus software. **c** T20 mock and T20 cells stably expressing UCHL1 were collected for transwell assay as described in the "Methods" section. The migrated cells were determined by counting five spots of each transwell and data are presented as mean ± S.D. **d** Immunoblot analysis of EMT markers on PM and T20 cells. Whole cell lysates were collected and extracted from PM and T20 cells, respectively. The expressions of EMT markers were determined by immunoblot assay through probing with E-cadherin, EpCAM, KRT 7, N-cadherin, and integrin β1/β3 antibodies. **e** Immunoblot analysis of EMT markers on T20 mock cells and T20 cells transfected with UCHL1. Whole cell lysates extracted from T20 mock cells and T20 cells stably expressing UCHL1 were subjected to immunoblot analysis using antibodies against fibronectin, integrin β1, and VIM. β-Actin was used as a loading control. The intensity of the bands for each blot was quantified by Gel-Pro Analyzer. Results are expressed as one representative out of three independent repeats, $*p \leq 0.05$; $**p \leq 0.01$

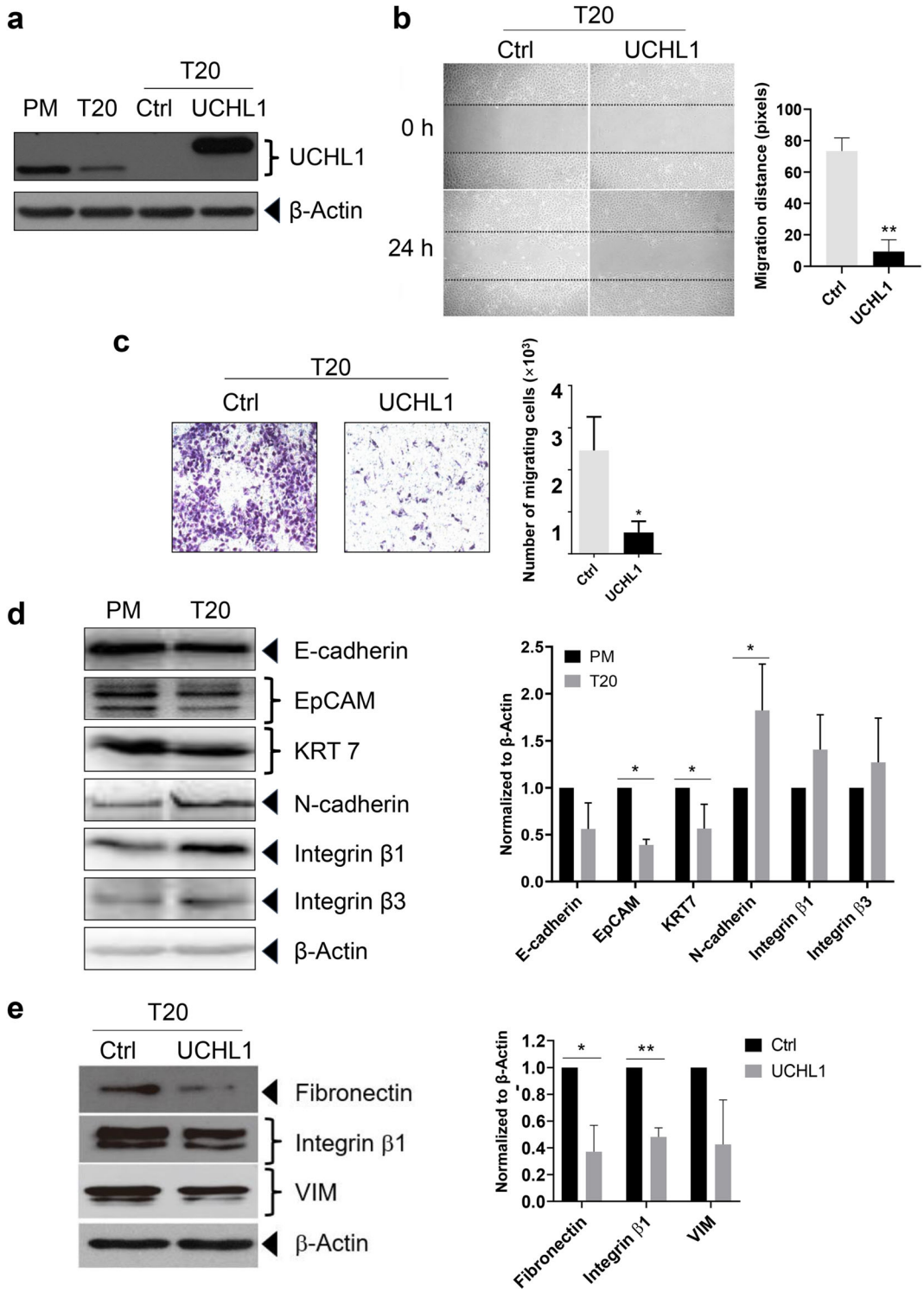
a
T20
PM T20 Ctrl UCHL1
UCHL1
β-Actin
b
T20
Ctrl UCHL1
0 h
24 h
Migration distance (pixels)
100
80
60
40
20
0
**
Ctrl
UCHL1
c
T20
Ctrl UCHL1
Number of migrating cells (×10³)
4
3
2
1
*
Ctrl
UCHL1
d
PM T20
E-cadherin
EpCAM
KRT 7
N-cadherin
Integrin β1
Integrin β3
β-Actin
Normalized to β-Actin
2.5
2.0
1.5
1.0
0.5
0.0
PM
T20
*
*
*
E-cadherin
EpCAM
KRT7
N-cadherin
Integrin β1
Integrin β3
e
T20
Ctrl UCHL1
Fibronectin
Integrin β1
VIM
β-Actin
Normalized to β-Actin
1.2
1.0
0.8
0.6
0.4
0.2
0.0
*
**
Ctrl
UCHL1
Fibronectin
Integrin β1
VIM

described, T20 cells exhibited EMT and enhanced cell migration (Liang et al. 2018). To investigate whether UCHL1 is a player in the enhanced T20 cell migration, we ectopically expressed UCHL1 back in T20 cells and performed scratch/transwell assay on T20 mock and UCHL1-transfected cells. We found that stable overexpression of UCHL1 in T20 cells dramatically decreased the number of migrated cells comparing to empty vector control as shown in both scratch assay (Fig. 4a, b) and transwell assay (Fig. 4c). These results are supportive of UCHL1 function in the suppression of cell migration.

UCHL1 expression is correlated to EMT

To further confirm the effects of UCHL1 on chronic Cd exposure-induced cell migration, immunoblot analysis of EMT markers was performed in T20 cells stably expressing UCHL1. The EMT markers were assessed in PM and T20 cells first. As shown in Fig. 4d and Fig. S3, the expression of epithelial markers (E-cadherin, EpCAM, and KRT7) were reduced, while the expression of mesenchymal markers, like N-cadherin, integrin β1/β3, VIM, and S100A11 were increased strongly, which is consistent to our previous results (Liang et al. 2018). Then, we examined the expression of EMT markers in T20 cells stably expressing UCHL1. The exogenous overexpression of UCHL1 suppressed mesenchymal marker expressions, such as fibronectin, integrin β1, and VIM (Fig. 4e). These results reveal that the deficiency of UCHL1 exacerbates Cd-transformed cell metastasis.

Restoring UCHL1 expression by epigenetic inhibitors in T20 cells

To explore how UCHL1 is dysregulated in Cd-transformed BEAS-2B cells and identify the transcriptional regulation of UCHL1, we first analyzed the UCHL1 mRNA expression in PM and T20 cells by RT-PCR and quantitative real-time RT-PCR. Results show that mRNA expression of UCHL1 decreased significantly in T20 cells compared to PM (Fig. 5a), which is consistent with the protein level (Fig. S3). Since small molecule epigenetic inhibitors are widely used to unravel the basic insights into epigenetic regulation and UCHL1 is consistently reported as silenced because of DNA methylation in the promoter, T20 cells were challenged with DNA methyltransferase inhibitor 5-Aza-dC. It is shown that T20 cells partially restored UCHL1 expression upon 5-Aza-dC treatment by immunoblot analysis (Fig. 5b). To further explore the epigenetic modulation of UCHL1 expression, histone deacetylase (HDAC) inhibitors were used. Notably, with the treatment of MS-275, a selective inhibitor for HDAC1–3, T20 cells re-expressed more than 50% of UCHL1 expression (Fig. 5c). This indicates that permanent changes had occurred in T20 cells, in which UCHL1 is likely to be epigenetically silenced by chronic Cd exposure. In addition, the epigenetic effects on the expression of UCHL1 were also observed in PBECs. UCHL1 expression was upregulated 5.5 times upon 5-Aza-dC treatment and 25 times with HDAC inhibitor TSA, a pan-HDAC inhibitor, compared with untreated control by quantitative real-time RT-PCR (Fig. 5d, e), which indicated that the suppression of UCHL1 was likely resulted from DNA methylation and histone deacetylation.

Ubiquitylome analysis of PM and T20 cells

UCHL1 is a key component in the ubiquitin-proteasome pathway through associating or releasing ubiquitin from cellular proteins. We asked whether T20 cells with silenced UCHL1 would lead to perturbed protein ubiquitylation levels. To examine the ubiquitylation changes in response to chronic Cd exposure, we ultilize an unbiased ubiquitin protein array which can simultaneously detect the ubiquitylation levels of 49 well-known cellular proteins. Overall, the perturbations of 23 ubiquitylated proteins was found in T20 cells (Fig. 6a). Among them, A20 (also known as TNFAIP3, a ubiquitin-editing enzyme) was the top-hit candidate protein with the greatest fold of increase in ubiquitylation levels, as compared with PM cells (with increase of 2.91-fold, Fig. 6a). Other proteins, such as Nrf2 (2.86-fold), IRF3 (2.54-fold), F-box protein 15 (2.52-fold), FGFR 2α/2β (2.42-fold), HGFR (2.38-fold), MSPR (2.30-fold), IκB-α (2.29-fold), CD44 (2.23-fold), ER-α (2.11-fold), HSP70 (1.86-fold), and p53 (1.83-fold) also showed increased levels of ubiquitylation (Fig. 6a). Furthermore, immunoblot analysis of some of the selected targets was performed to confirm the array results. In Fig. 6b, we showed that the elevated spot intensity in array, indicating increased ubiquitylation levels, corresponded to reduced protein expression (such as p53, and IκB-α). These results likely support that the silencing of UCHL1 during a Cd-induced BEAS-2B cell transformation also leads to the perturbation of ubiquitin homeostasis in T20 cells, leading to reduced levels of tumor suppressor like

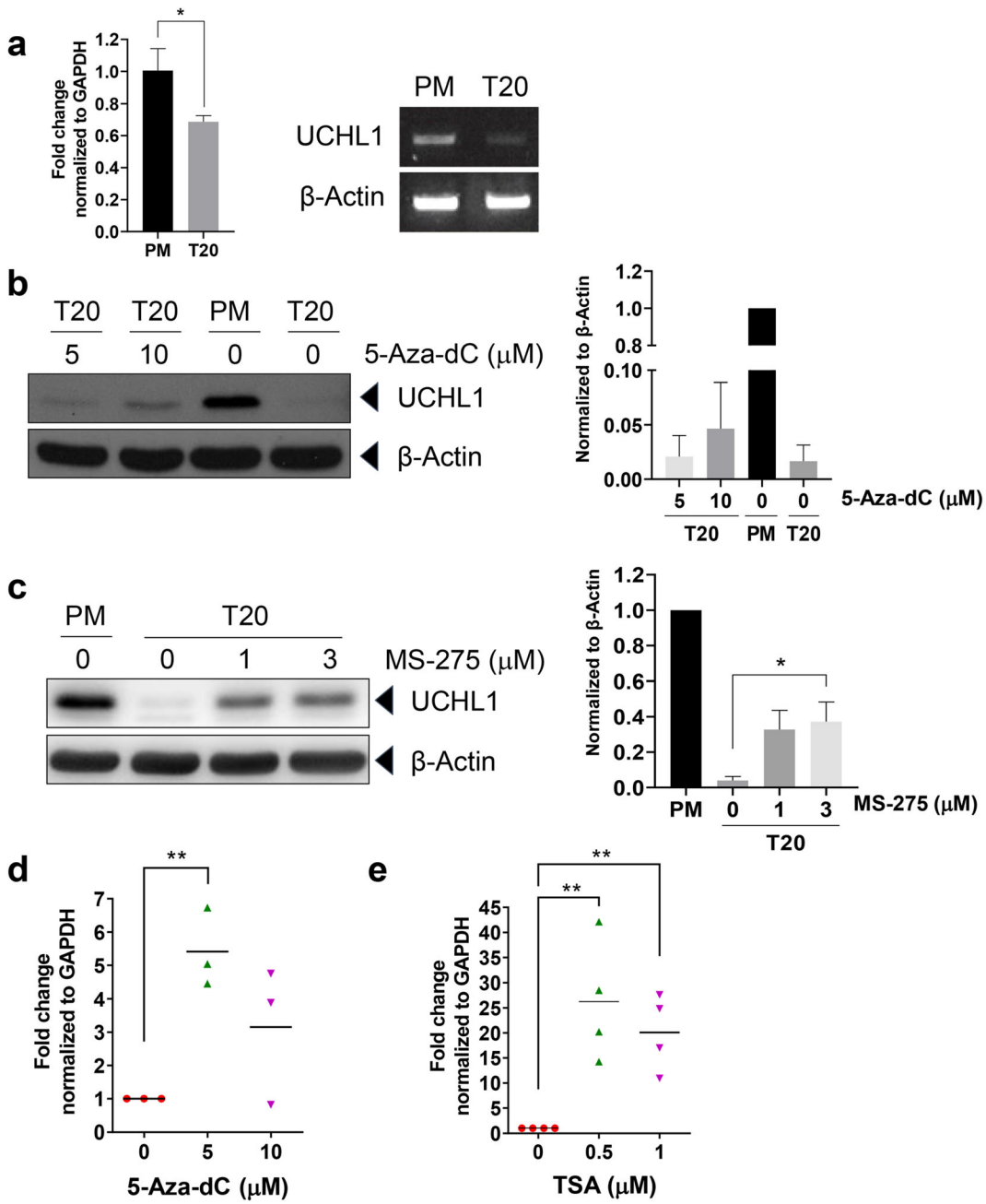

Fig. 5 Restoring UCHL1 expression by epigenetic inhibitors. **a** Expression of UCHL1 level in PM and T20 cells was amplified using quantitative real-time RT-PCR (left) and RT-PCR (right), with GAPDH and β-actin as an internal control, respectively. **b**, **c** Immunoblot analysis of UCHL1 level in T20 cells treated with epigenetic inhibitors. T20 cells were sham-exposed or challenged with 5–10 μM of 5-Aza-dC **b** or 1–3 μM of MS-275 **c** for 48 h, respectively. Cells were collected and subjected to immunoblot assay using UCHL1 antibody. β-Actin was used as a loading control. The intensity of the bands for each blot were quantified by Gel-Pro Analyzer. **d**, **e** Quantitative real-time RT-PCR analysis of UCHL1 expression in PBECs exposed to epigenetic inhibitors. PBECs were sham-exposed or treated with 5–10 μM of 5-Aza-dC **d** or 0.5–1 μM of TSA **e** for 24 h, respectively. Cells were harvested for RNA isolation and quantitative real-time RT-PCR was used to determine the mRNA level of UCHL1. GAPDH was used as an internal control. Data are expressed as mean with three **d** or four **e** independent repeats, $*p \leq 0.05$; $**p \leq 0.01$

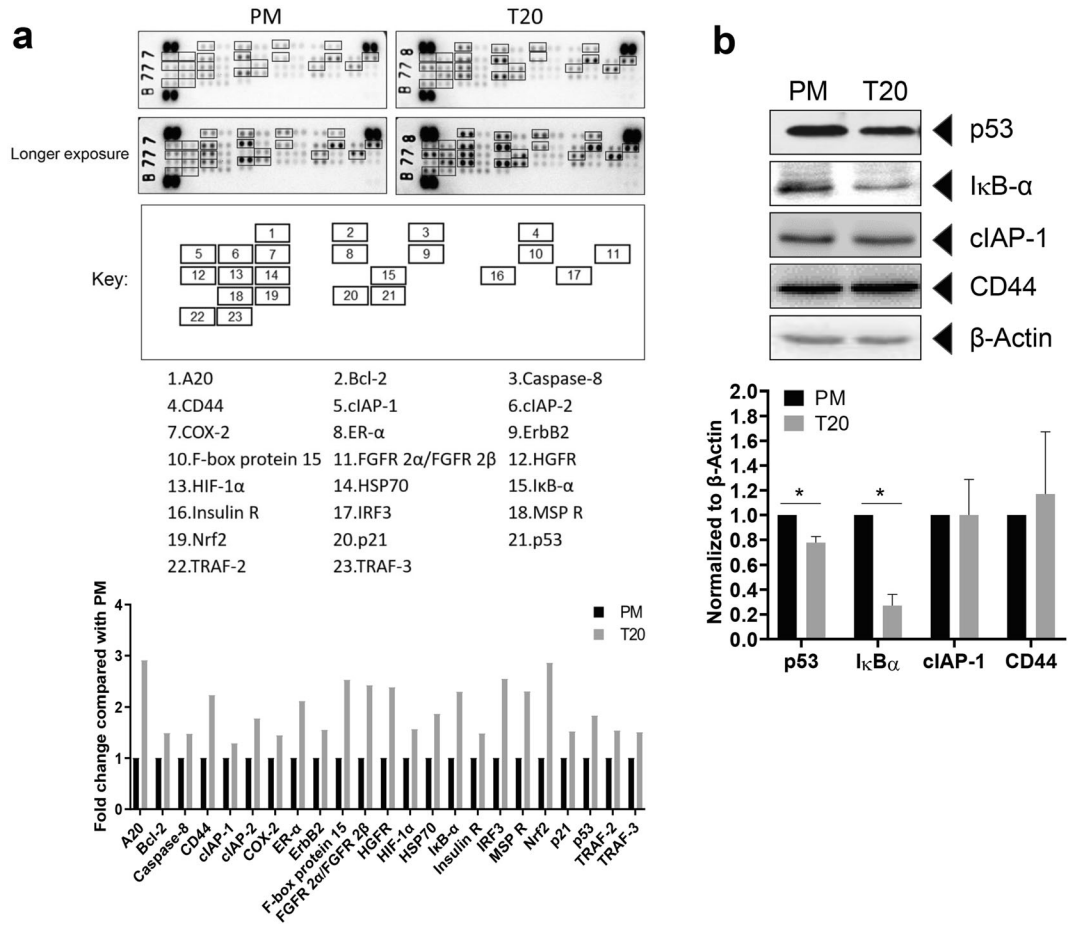

Fig. 6 Ubiquitylome analysis of PM and T20 cells. **a** Cell lysates extracted from PM and T20 cells were subjected to the human ubiquitin array kit following manufacturer's instructions. Each dot represents the ubiquitylation level of an indicated protein detected by an anti-ubiquitin antibody. Data are shown in fold change normalized to PM. **b** Immunoblot analysis for verifying the expression level of some selected target proteins from **a.** Cell lysates extracted from PM and T20 cells were subjected to SDS-PAGE followed by immunoblot assay using antibodies against p53, IκB-α, cIAP-1, and CD44. β-Actin was monitored as a loading control. The intensity of the bands for each blot were quantified by Gel-Pro Analyzer, $*p \leq 0.05$

p53 and some other cell cycle check point or DNA repair proteins.

Discussion

We systematically examined for the first time the subproteome alterations in chronic Cd-challenged human bronchial epithelial cells in this study, and identified a total of 63 differentially expressed proteins between Cd-transformed and PM control cells. In particular, UCHL1 was dramatically downregulated in Cd-transformed cells, and the silencing of UCHL1 may be regulated by epigenetic mechanisms. Notably, the EMT phenotype of Cd-transformed cells can be reverted through forced ectopic expression of UCHL1. We also explored the ubiquitylation changes upon chronic Cd exposure and results showed that perturbation of 23 ubiquitylated proteins was found in Cd-transformed cells.

UCHL1, a member of the UCH family, functions to maintain ubiquitin balance by associating or releasing ubiquitin from cellular proteins through the proteasome pathway. UCHL1 was abundantly expressed in the neuronal tissues and involved in neurodegenerative diseases, but also found to be abnormally expressed in multiple cancers (Mandelker et al. 2005; Okochi-Takada et al. 2006; Yamashita et al. 2006; Kagara et al. 2008; Tokumaru et al. 2008; Yu et al. 2008; Li et al. 2010; Ummanni et al. 2011; Jin et al. 2013; Tian et al. 2013; Abdelmaksoud-Dammak et al. 2016; Liu et al. 2020; Zhao et al. 2020). Currently, the

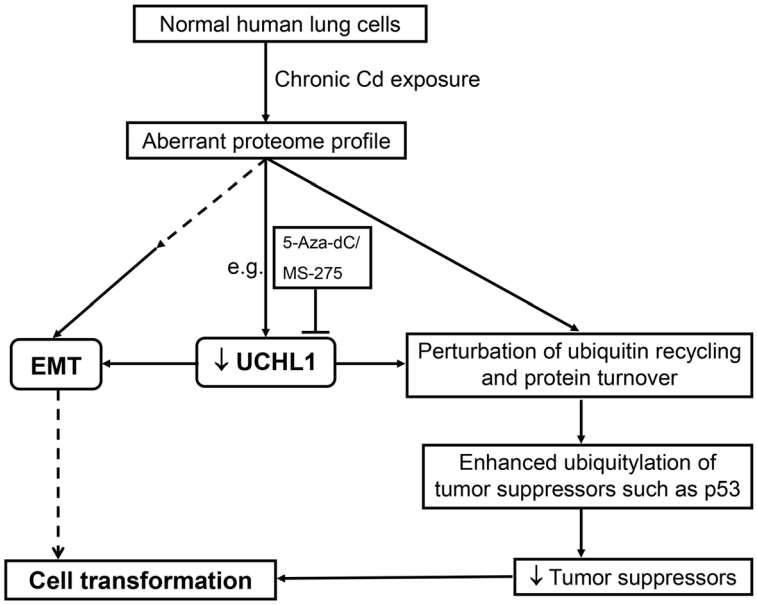

Fig. 7 A model of Cd action based on our data is presented. Chronic exposure of normal human bronchial epithelial BEAS-2B cells to $CdCl_2$ can lead to perturbation of cellular subproteomes and ubiquitylome, causing the aberrant levels of tumor suppressors and oncogenes. UCHL1 may play a function in the suppression of EMT in Cd-transformed human lung epithelial cells, indicating that UCHL1 might be a new therapeutic target for chronic Cd-induced carcinogenesis

role of UCHL1 in tumorigenesis is controversial: It has been reported as either a tumor suppressor or an oncogene, which depends on the cancer types. DNA methylation in the UCHL1 promoter, leading to the silencing of UCHL1, has been frequently reported in several cancers, supporting the role of UCHL1 as a tumor suppressor, such as nasopharyngeal (Li et al. 2010; Tian et al. 2013; Zhao et al. 2020), esophageal (Mandelker et al. 2005), gastric (Yamashita et al. 2006), renal (Kagara et al. 2008), head and neck squamous cell carcinoma (Tokumaru et al. 2008), hepatocellular (Yu et al. 2008), ovarian (Jin et al. 2013; Okochi-Takada et al. 2006), prostate (Ummanni et al. 2011), and colorectal cancers (Abdelmaksoud-Dammak et al. 2016). However, the function of UCHL1 in lung-related disease is ambiguous.

Based on our results, the loss of UCHL1 expression in Cd-transformed cells likely contributed to the EMT phenotype, as ectopic expression of UCHL1 back in Cd-transformed cells effectively suppress the expression of EMT marker proteins and cell migration ability of these cells. These findings are consistent with a recent report showing that overexpression of UCHL1 significantly suppressed cell migration and invasion of nasopharyngeal carcinoma (Zhao et al. 2020). In addition, we demonstrated that UCHL1 was epigenetically silenced in the Cd-transformed cells. The silencing of UCHL1 was likely caused by DNA hypermethylation and histone deacetylation, since 5-Aza-dC and MS-275 could partially revert the expression of UCHL1 in T20 cells. Sufficient evidences have indicated that the silencing of UCHL1 is closely associated with DNA methylation in the promoter, but little is known about the effects of histone deacetylation on the regulation of UCHL1. In the current study, we found that UCHL1 could be re-expressed upon histone deacetylase inhibitor MS-275 treatment, and this was also validated in PBECs exposed to TSA. Although these findings provide basic insights into the epigenetic regulation of UCHL1 expression, the underlying epigenetic modulation of UCHL1 still needs further exploration.

The silenced UCHL1 in T20 cells would lead to the perturbation of ubiquitin recycling and protein turnover in T20 cells. UCHL1 has been shown to both enhance or reduce the ubiquitylation level of proteins, a case in point is the ability of UCHL1 to ubiquitylate MDM2 but deubiquitylate p53 and $p14^{ARF}$, which lead to MDM2 degradation but stabilization of p53 and $p14^{ARF}$ (Li et al. 2010). Although it is yet to be determined if there is a connection of UCHL1 to the ubiquitylation level of the other 62 protein types that we identified on 2-DE gels as well as those examined EMT marker proteins in this work, we hypothesize that some of these targets are likely to be regulated by UCHL1, especially for those proteins that are known to be degraded through the proteasomal pathways. To further investigate if the reduced UCHL1 in T20 cells would lead to perturbed protein ubiquitylation levels, we utilized the ubiquitin protein array which can simultaneously detect the ubiquitylation levels of 49 well-known cellular proteins. From the antibody array results, we found that most of the protein targets had higher levels

of ubiquitylation, which would likely correlate with enhanced turnover/degradation of these proteins. This assumption can be proven by the results obtained from subsequent immunoblot analysis, which is in agreement of the fact that protein targets on the antibody array with higher ubiquitylation level correspond with reduced protein amounts, such as the tumor suppressor p53. Overall, we believe that Cd, by epigenetic silencing of UCHL1, would likely lead to perturbation of a spectrum of proteins inside the cells. It will be tempting to further study the ubiquitylome of T20 cells to see how many more ubiquitylated proteins are affected as a result of chronic Cd exposure.

In summary, we believe that UCHL1 is a master regulator of protein turnover in the cells, and it is unprecedented that chronic Cd exposure would lead to epigenetic silencing of UCHL1 (Fig. 7). Our data report for the first time that UCHL1 may play a function in the suppression of EMT in Cd-transformed human lung epithelial cells. Therefore, restoring the expression of UCHL1 might be beneficial for targeting those cancers (e.g., Cd-induced lung cancers) with silenced UCHL1 expression.

Acknowledgments We would like to thank members of the Lau And Xu laboratory for critical reading of this manuscript and also Prof. dr. Irene Heijink, University Medical Center Groningen, the Netherlands for providing the PBECs.

Funding This work was supported by the grants from the National Natural Science Foundation of China (Nos. 31771582 and 31170785); the Guangdong Natural Science Foundation of China (No. 2017A030313131); the "Thousand, Hundred, and Ten" project of the Department of Education of Guangdong Province of China, the Basic and Applied Research Major Projects of Guangdong Province of China (2017KZDXM035 and 2018KZDXM036); the "Yang Fan" Project of Guangdong Province of China (Andy T. Y. Lau-2016; Yan-Ming Xu-2015); and the Abel Tasman Talent Program at the University Medical Center Groningen, the Netherlands.

Compliance with ethical standards

Conflict of interest The authors declare that they have no conflict of interest.

References

Abdelmaksoud-Dammak R, Saadallah-Kallel A, Miladi-Abdennadher I, Ayedi L, Khabir A, Sallemi-Boudawara T, et al. CpG methylation of ubiquitin carboxyl-terminal hydrolase 1 (UCHL1) and P53 mutation pattern in sporadic colorectal cancer. Tumour Biol. 2016;37(2):1707–14.

Ganguly K, Levanen B, Palmberg L, Akesson A, Linden A. Cadmium in tobacco smokers: a neglected link to lung disease? Eur Respir Rev. 2018;27(147):170122.

Gao Y, Xu Y, Wu D, Yu F, Yang L, Yao Y, et al. Progressive silencing of the zinc transporter Zip8 (Slc39a8) in chronic cadmium-exposed lung epithelial cells. Acta Biochim Biophys Sin. 2017;49(5):444–9.

International Agency for Research on Cancer. IARC monographs on the evaluation of the carcinogenic risks to humans: beryllium, cadmium, mercury, and exposures in the glass manufacturing industry. IARC. 1993;58:119–238.

Jin C, Yu W, Lou X, Zhou F, Han X, Zhao N, et al. UCHL1 is a putative tumor suppressor in ovarian cancer cells and contributes to cisplatin resistance. J Cancer. 2013;4(8):662–70.

Kagara I, Enokida H, Kawakami K, Matsuda R, Toki K, Nishimura H, et al. CpG hypermethylation of the UCHL1 gene promoter is associated with pathogenesis and poor prognosis in renal cell carcinoma. J Urol. 2008;180(1):343–51.

Kawasaki T, Kono K, Dote T, Usuda K, Shimizu H, Dote E. Markers of cadmium exposure in workers in a cadmium pigment factory after changes in the exposure conditions. Toxicol Ind Health. 2004;20(1-5):51–6.

Kim HS, Kim YJ, Seo YR. An overview of carcinogenic heavy metal: molecular toxicity mechanism and prevention. J Cancer Prev. 2015;20(4):232–40.

Kirschvink N, Martin N, Fievez L, Smith L, Marlin D, Gustin P. Airway inflammation in cadmium-exposed rats is associated with pulmonary oxidative stress and emphysema. Free Radic Res. 2006;40(3):241–50.

Lau ATY, Chiu JF. The possible role of cytokeratin 8 in cadmium-induced adaptation and carcinogenesis. Cancer Res. 2007;67(5):2107–13.

Lee YH, Tan HT, Chung MC. Subcellular fractionation methods and strategies for proteomics. Proteomics. 2010;10(22):3935–56.

Li L, Tao Q, Jin H, van Hasselt A, Poon FF, Wang X, et al. The tumor suppressor UCHL1 forms a complex with p53/MDM2/ARF to promote p53 signaling and is frequently silenced in nasopharyngeal carcinoma. Clin Cancer Res. 2010;16(11):2949–58.

Liang ZL, Wu DD, Yao Y, Yu FY, Yang L, Tan HW, et al. Epiproteome profiling of cadmium-transformed human bronchial epithelial cells by quantitative histone post-translational modification-enzyme-linked immunosorbent assay. J Appl Toxicol. 2018;38(6):888–95.

Liu SJ, Gonzalez-Prieto R, Zhang MD, Geurink PP, Kooij R, Iyengar PV, et al. Deubiquitinase activity profiling identifies UCHL1 as a Candidate oncoprotein that promotes tgf beta-induced breast cancer metastasis. Clin Cancer Res. 2020;26(6):1460–73.

Livak KJ, Schmittgen TD. Analysis of relative gene expression data using real-time quantitative PCR and the 2-ΔΔCT Method. Methods. 2001;25:402–8.

Mandelker DL, Yamashita K, Tokumaru Y, Mimori K, Howard DL, Tanaka Y, et al. PGP9.5 promoter methylation is an independent prognostic factor for esophageal squamous cell carcinoma. Cancer Res. 2005;65(11):4963–8.

Nair AR, DeGheselle O, Smeets K, Van Kerkhove E, Cuypers A. Cadmium-Induced pathologies: where is the oxidative balance lost (or not)? Int J Mol Sci. 2013;14(3):6116–43.

Okochi-Takada E, Nakazawa K, Wakabayashi M, Mori A, Ichimura S, Yasugi T, et al. Silencing of the UCHL1 gene in human colorectal and ovarian cancers. Int J Cancer. 2006;119(6):1338–44.

Satarug S, Moore MR. Adverse health effects of chronic exposure to low-level cadmium in foodstuffs and cigarette smoke. Environ Health Perspect. 2004;112(10):1099–103.

Scherer G, Barkemeyer H. Cadmium concentrations in tobacco and tobacco smoke. Ecotoxicol Environ Saf. 1983;7(1):71–8.

Tan HW, Xu YM, Wu DD, Lau ATY. Recent insights into human bronchial proteomics - how are we progressing and what is next? Expert Rev Proteomics. 2018;15(2):113–30.

Tan HW, Liang ZL, Yao Y, Wu DD, Mo HY, Gu J, et al. Lasting DNA damage and aberrant DNA repair gene expression profile are associated with post-chronic cadmium exposure in human bronchial epithelial cells. Cells. 2019;8(8):842.

Tian F, Yip SP, Kwong DL, Lin Z, Yang Z, Wu VW. Promoter hypermethylation of tumor suppressor genes in serum as potential biomarker for the diagnosis of nasopharyngeal carcinoma. Cancer Epidemiol. 2013;37(5):708–13.

Tokumaru Y, Yamashita K, Kim MS, Park HL, Osada M, Mori M, et al. The role of PGP9.5 as a tumor suppressor gene in human cancer. Int J Cancer. 2008;123(4):753–9.

Ummanni R, Jost E, Braig M, Lohmann F, Mundt F, Barett C, et al. Ubiquitin carboxyl-terminal hydrolase 1 (UCHL1) is a potential tumour suppressor in prostate cancer and is frequently silenced by promoter methylation. Mol Cancer. 2011;10:129.

World Health Organization (WHO). Exposure to cadmium: a major public health concern. Geneva: WHO; 2010.

Xu YM, Tan HW, Zheng W, Liang ZL, Yu FY, Wu DD, et al. Cadmium telluride quantum dot-exposed human bronchial epithelial cells: a further study of the cellular response by proteomics. Toxicol Res. 2019;8(6):994–1001.

Yamashita K, Park HL, Kim MS, Osada M, Tokumaru Y, Inoue H, et al. PGP9.5 methylation in diffuse-type gastric cancer. Cancer Res. 2006;66(7):3921–7.

Yu J, Tao Q, Cheung KF, Jin H, Poon FF, Wang X, et al. Epigenetic identification of ubiquitin carboxyl-terminal hydrolase L1 as a functional tumor suppressor and biomarker for hepatocellular carcinoma and other digestive tumors. Hepatology. 2008;48(2):508–18.

Zhao Y, Lei Y, He SW, Li YQ, Wang YQ, Hong XH, et al. Hypermethylation of UCHL1 promotes metastasis of nasopharyngeal carcinoma by suppressing degradation of cortactin (CTTN). Cells. 2020;9(3):559.